



Attitude Estimation Based on Multi-Frequency Motion Modeling and Complementary Filtering Using Inertial Sensor Data

Hoang Van Ngoi^{1*}

¹Missile Faculty, Air Defence-Air Force Academy, Ha Noi, Viet Nam

*Corresponding author email: hoangngoi1992@gmail.com

DOI: <https://doi.org/10.63680/ijstate0526007.7>

Abstract

This paper presents a method for estimating the Euler angles (roll, pitch, yaw) of a ship through simulation of data from a multi-frequency wave model and processing by a complementary filter. The multi-frequency wave model is employed to reconstruct the actual oscillatory trajectory of the ship at sea, combined with simulated inertial measurement unit (IMU) data including accelerometers and gyroscopes, taking into account random noise and systematic errors. The Euler angles are estimated by integrating gyro data and by a complementary filter that combines gyroscope and accelerometer measurements. Simulation results show that the complementary filter reduces estimation errors compared with the gyro-only method, while enhancing the stability of the angle signals under sensor noise conditions. The proposed method can be applied in ship navigation and control systems operating in rough sea environments.

Keywords: Euler angle estimation; IMU; ship; multi-frequency wave model; complementary filter; inertial sensors; signal filtering.

1. Introduction

In the maritime field, accurate determination of ship attitude (roll, pitch, yaw) plays a crucial role in control, navigation, and stabilization systems. Inertial measurement units (IMUs) are commonly used to measure angular velocity and linear acceleration, from which Euler angles are calculated. However, in rough sea conditions, IMU data are strongly affected by sensor noise, bias drift, and wave-induced oscillations, leading to significant errors if only a single type of sensor is used.

The multi-frequency wave model is an effective tool to simulate the actual motion of a ship, consisting of multiple wave components with different amplitudes, frequencies, and phases. Combining this simulated data with signal processing algorithms allows evaluation and improvement of estimation methods. In this paper, the authors propose using a complementary filter to exploit the advantages of gyroscopes (fast response, short-term stability) and accelerometers (long-term stability) in order to minimize errors and improve reliability of the results.

2. Algorithm Synthesis

The motion of a ship under rough sea conditions is described by three actual Euler angles $\phi(t)$ (roll), $\theta(t)$ (pitch) and $\psi(t)$ (yaw). Each angle is the sum of multiple independent harmonic wave components:

$$x_{true} = \sum_{i=1}^{n_x} A_{x,i} \sin\left(\frac{2\pi}{T_{x,i}}t + \varphi_{x,i}\right) \tag{1}$$

With: $x \in \{\phi, \theta, \psi\}$.

$$\phi_{true}(t) = \sum_{i=1}^{n_\phi} A_{\phi,i} \sin\left(\frac{2\pi}{T_{\phi,i}}t + \varphi_{\phi,i}\right) \tag{2}$$

$$\theta_{true}(t) = \sum_{i=1}^{n_\theta} A_{\theta,i} \sin\left(\frac{2\pi}{T_{\theta,i}}t + \varphi_{\theta,i}\right) \tag{3}$$

$$\psi_{true}(t) = \sum_{i=1}^{n_\psi} A_{\psi,i} \sin\left(\frac{2\pi}{T_{\psi,i}}t + \varphi_{\psi,i}\right) \tag{4}$$

Where:

$A_{x,i}$: amplitude of the i-th wave component (rad);

$T_{x,i}$: period of the i-th wave component (s);

$\varphi_{x,i}$: initial phase (rad);

$\phi_{true}(t), \theta_{true}(t), \psi_{true}(t)$: true Euler angles at time t (rad).

- To relate the angular velocity of the ship body to the time derivatives of the Euler angles, the kinematic transformation matrix is used. The relationship between the body angular velocity vector $[p, q, r]^T$ and Euler angle derivatives is expressed as:

$$\begin{bmatrix} p \\ q \\ r \end{bmatrix} = T(\phi, \theta) \begin{bmatrix} \dot{\phi} \\ \dot{\theta} \\ \dot{\psi} \end{bmatrix} \tag{5}$$

Where:

p, q, r : angular velocities about the body axes (rad/s);

$T(\phi, \theta)$: transformation matrix from Euler angle rates to body angular velocity vector;

ϕ, θ, ψ : Euler angles (rad);

$\dot{\phi}, \dot{\theta}, \dot{\psi}$: Euler angle rates (rad/s).

- The transformation matrix has the form:

$$T(\phi, \theta) = \begin{bmatrix} 1 & 0 & -\sin \theta \\ 0 & \cos \phi & \sin \phi \cos \theta \\ 0 & -\sin \phi & \cos \phi \cos \theta \end{bmatrix} \tag{6}$$

- Substituting the true Euler angle derivatives into (5), the ideal angular velocity of the ship is obtained:

$$\omega_{true}(t) = \begin{bmatrix} p_{true}(t) \\ q_{true}(t) \\ r_{true}(t) \end{bmatrix} = \mathbf{T}(\phi_{true}, \theta_{true}) \begin{bmatrix} \dot{\phi}_{true}(t) \\ \dot{\theta}_{true}(t) \\ \dot{\psi}_{true}(t) \end{bmatrix} \tag{7}$$

- To describe the orientation relationship between the inertial coordinate system and the body coordinate system, the Direction Cosine Matrix (DCM) is used. With the Z-Y-X rotation sequence (yaw-pitch-roll), the transformation matrix from inertial frame n to body frame b is:

$$\mathbf{C}_{nb} = \mathbf{R}_x(\phi) \mathbf{R}_y(\theta) \mathbf{R}_z(\psi) \tag{8}$$

With the rotation matrices about each axis as follows:

$$\mathbf{R}_x(\phi) = \begin{bmatrix} 1 & 0 & 0 \\ 0 & \cos \phi & \sin \phi \\ 0 & -\sin \phi & \cos \phi \end{bmatrix} \tag{9}$$

$$\mathbf{R}_y(\theta) = \begin{bmatrix} \cos \theta & 0 & -\sin \theta \\ 0 & 1 & 0 \\ \sin \theta & 0 & \cos \theta \end{bmatrix} \tag{10}$$

$$\mathbf{R}_z(\psi) = \begin{bmatrix} \cos \psi & \sin \psi & 0 \\ -\sin \psi & \cos \psi & 0 \\ 0 & 0 & 1 \end{bmatrix} \tag{11}$$

$\mathbf{R}_x, \mathbf{R}_y, \mathbf{R}_z$:are rotation matrices around axes x, y, z (dimensionless).

- Based on the direction cosine matrix, the ideal accelerometer signals can be calculated. When only gravitational acceleration acts, the acceleration vector in the inertial frame is $[0, 0, g]^T$. The accelerometer in the body frame measures:

$$\mathbf{a}_{ideal}(t) = \mathbf{C}_{nb}^T(\phi, \theta, \psi) \begin{bmatrix} 0 \\ 0 \\ g \end{bmatrix} \tag{12}$$

$\mathbf{a}_{ideal}(t)$: ideal accelerometer signal in the body frame b (m/s^2);

g : gravitational acceleration (m/s^2);

$\mathbf{C}_{nb}^T(\phi, \theta, \psi)$: direction cosine matrix from inertial frame n to body frame b (dimensionless).

- In practice, sensor data are imperfect and always contain systematic error (bias) and random noise. Thus, the measured accelerometer and gyroscope data are modeled as follows:

$$\mathbf{a}_{meas}(t) = \mathbf{a}_{ideal}(t) + \mathbf{b}_a + \mathbf{n}_a(t) \tag{13}$$

$$\omega_{meas}(t) = \omega_{true}(t) + \mathbf{b}_g + \mathbf{n}_g(t) \tag{14}$$

To estimate angles from the accelerometer, the signal is first low-pass filtered to remove high-frequency noise, then calculated as:

$$\phi_{acc}(t) = \arctan \frac{a_y(t)}{a_z(t)} \tag{15}$$

$$\theta_{acc}(t) = \arctan \left(\frac{-a_x(t)}{\sqrt{a_y^2(t) + a_z^2(t)}} \right) \quad (16)$$

Meanwhile, the gyroscope allows updating the attitude quaternion from the measured angular velocity vector:

$$\dot{q}(t) = \frac{1}{2} \Omega(\omega_{meas}(t)) \cdot q(t) \quad (17)$$

With the matrix:

$$\Omega(\omega) = \begin{bmatrix} 0 & -p & -q & -r \\ p & 0 & r & -q \\ q & -r & 0 & p \\ r & q & -p & 0 \end{bmatrix} \quad (18)$$

From the quaternion, the direction cosine matrix can be derived:

$$C_{nb} = \begin{bmatrix} q_0^2 + q_1^2 - q_2^2 - q_3^2 & 2(q_1q_2 + q_0q_3) & 2(q_1q_3 - q_0q_2) \\ 2(q_1q_2 - q_0q_3) & q_0^2 - q_1^2 + q_2^2 - q_3^2 & 2(q_2q_3 + q_0q_1) \\ 2(q_1q_3 + q_0q_2) & 2(q_2q_3 - q_0q_1) & q_0^2 - q_1^2 - q_2^2 + q_3^2 \end{bmatrix} \quad (19)$$

From which the Euler angles are extracted:

$$\phi_{gyro} = \arctan 2(C_{32}, C_{33}) \quad (20)$$

$$\theta_{gyro} = -\arcsin(C_{31}) \quad (21)$$

$$\psi_{gyro} = \arctan 2(C_{21}, C_{11}) \quad (22)$$

To combine the advantages of the gyro (short-term stability) and the accelerometer (long-term stability), the Complementary Filter (CF) is applied:

$$\phi_{CF}(t) = \alpha \phi_{gyro}(t) + (1 - \alpha) \phi_{acc}(t) \quad (23)$$

$$\theta_{CF}(t) = \alpha \theta_{gyro}(t) + (1 - \alpha) \theta_{acc}(t) \quad (24)$$

$$\psi_{CF}(t) = \psi_{gyro}(t) \quad (25)$$

Finally, to evaluate the estimation performance, the angle error is defined as the difference between estimated angle and true angle.

For the gyro-only case:

$$e_{gyro}(t) = \begin{bmatrix} \phi_{gyro} - \phi_{true} \\ \theta_{gyro} - \theta_{true} \\ \psi_{gyro} - \psi_{true} \end{bmatrix} \quad (26)$$

And for the complementary filter:

$$e_{CF}(t) = \begin{bmatrix} \phi_{CF} - \phi_{true} \\ \theta_{CF} - \theta_{true} \\ \psi_{CF} - \psi_{true} \end{bmatrix} \quad (27)$$

3. Simulation and Evaluation

To verify the effectiveness of the developed Euler angle estimation algorithm, the true ship trajectory is

generated by the multi-frequency wave model, and IMU sensor data are produced from the ideal model with added noise and bias errors. The Euler angles are estimated by two methods: gyro integration (gyro-only) and complementary filter (CF). The simulation parameters are selected as follows:

Sampling frequency: 200(Hz), simulation time: 100(s);

- Gravitational acceleration: $g=9.80665(m/s^2)$;

- Multi-frequency wave model:

Roll: amplitudes [12, 5, 3](deg); periods [10, 6, 3](s); phases $[0, \pi/4, -\pi/3]$;

Pitch: amplitudes [8, 4, 2](deg); periods [12, 8, 4](s); phases $[\pi/6, -\pi/5, \pi/2]$;

Yaw: amplitudes [4, 2](deg); periods [30,15](s); phases $[0, -\pi/6]$.

- Sensor errors and noise:

Accelerometer: bias [0.003, -0.002, 0.002]g; white noise RMS = 0.01g.

Gyroscope: bias [0.05, -0.04, 0.03] (deg/s); white noise RMS =0.03 (deg/s).

- Signal processing filters:

Accelerometer filtering: 4th-order Butterworth, cutoff frequency 5(Hz).

Angle smoothing from accelerometer: 2nd-order Butterworth, cutoff frequency 2(Hz).

- Complementary filter: weighting factor $\alpha=0.98$.

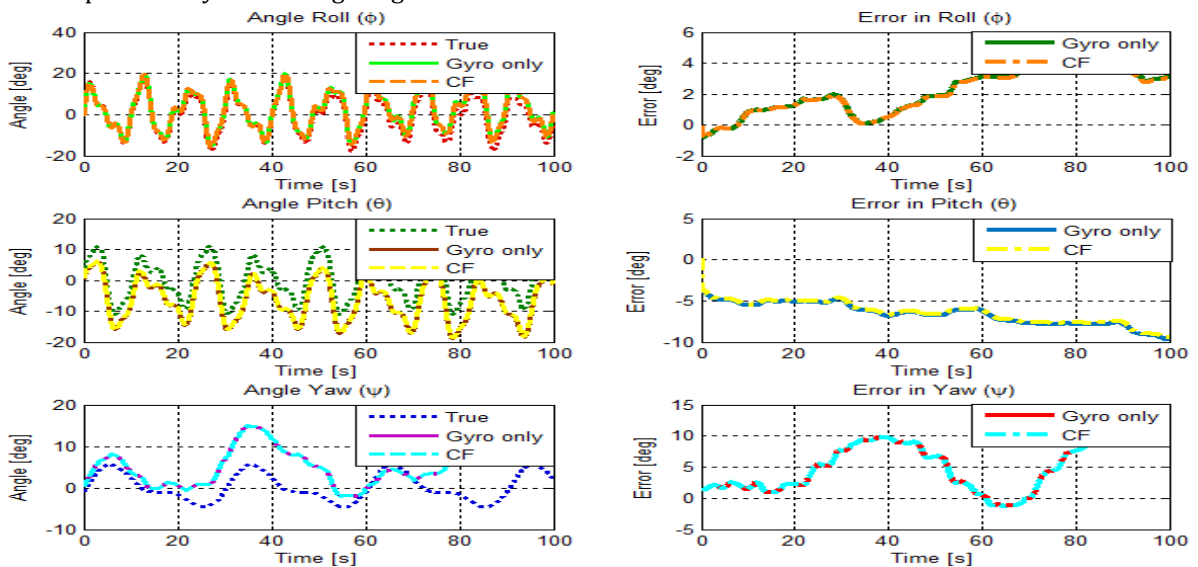


Figure 1. Euler angles and estimation errors using Gyro-only and Complementary Filter (CF)

Figure 1 illustrates the evolution of the three Euler angles (roll, pitch, yaw) of the ship and the corresponding estimation errors. The left column shows the true angles compared with estimation results from gyro-only and CF; the right column shows the errors of each method.

For roll (ϕ), both methods closely follow the true trajectory in the short term; however, gyro-only exhibits gradual drift over time. CF reduces this drift and maintains errors within ± 2 (deg).

For pitch (θ), gyro-only tends to deviate increasingly from the true value, especially as simulation time increases. CF provides more stable results, keeping errors below 5(deg), reflecting the advantage of accelerometer-based correction.

For yaw (ψ), since no accelerometer information is available, both gyro-only and CF rely solely on gyroscope data, so the error grows with time. Drift becomes significant after 50(s), reaching nearly 15(deg)

at the end of simulation.

The results in Figure 1 show that the CF method significantly improves the accuracy of roll and pitch, while yaw remains strongly affected by gyro error. This is consistent with the paper’s orientation: the complementary filter is a simple but effective solution in rough sea environments and can be extended by integrating magnetometer data to correct yaw.

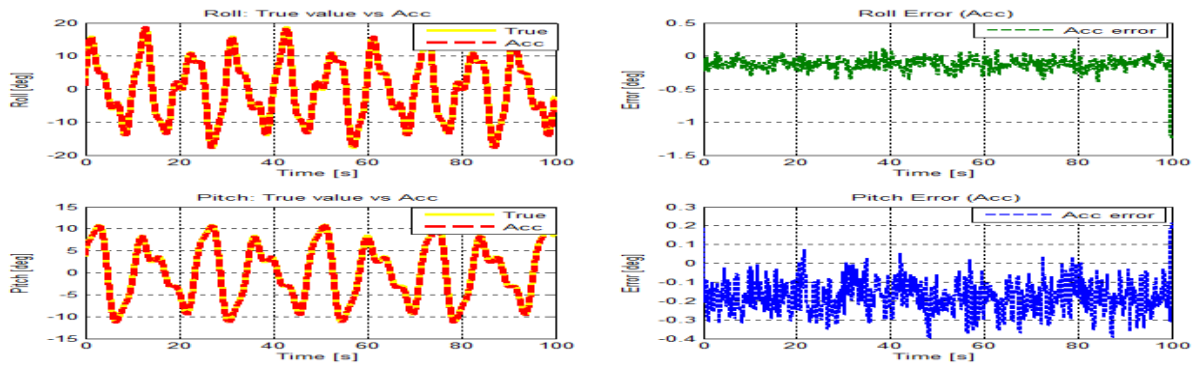


Figure 2. Roll and Pitch angles computed from accelerometer and errors relative to true values

Figure 2 compares roll (ϕ) and pitch (θ) estimated directly from accelerometer data with the true values. The left column shows the evolution of the two angles, while the right column shows the corresponding errors.

For roll, the accelerometer signal closely follows the true trajectory, with errors smaller than 1(deg). The error oscillates around zero, indicating that the accelerometer provides accurate long-term information.

For pitch, the results are similar; errors are mostly within $\pm 0.3(\text{deg})$, showing that the accelerometer-based angle computation is quite stable.

1. However, high-frequency noise oscillations appear in accelerometer data, even though the error amplitude is small. This confirms the necessity of low-pass filtering in sensor signal processing to remove noise while preserving correct trends. Overall, Figure 2 demonstrates that the accelerometer is an important source of information for correcting gyro drift, especially in the complementary filter, thereby significantly improving Euler angle estimation accuracy in rough sea environments.

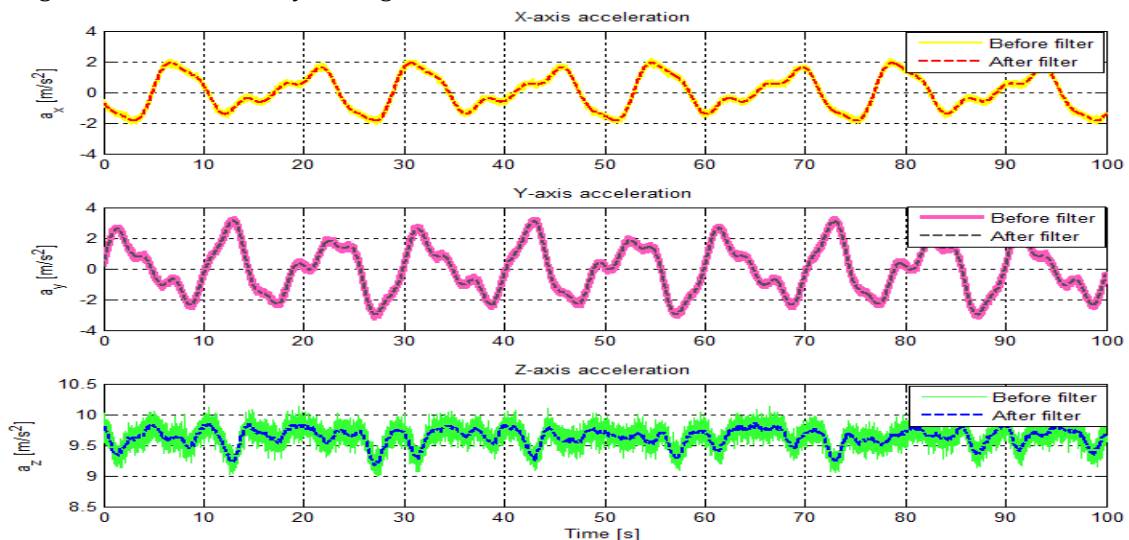


Figure 3. Accelerometer signals before and after filtering on three axes

Figure 3 shows acceleration signals along the three body axes, including data before filtering (Before filter) and after filtering (After filter).

On the x and y axes, pre-filter signals contain significant high-frequency noise oscillations superimposed on the main waveform. After applying a 4th-order Butterworth filter with cutoff frequency 5 Hz, noise components are greatly removed, leaving a smoother and more accurate oscillatory waveform.

On the z axis, acceleration oscillates around the value of g ; however, the pre-filter data show noticeable noise. After filtering, the signal is more stable, closely following gravity trend and actual ship oscillation.

The results in Figure 3 confirm the effectiveness of sensor data preprocessing: the low-pass filter smooths signals, reduces random noise influence, while preserving motion dynamics. This is crucial for accurate Euler angle computation from the accelerometer, and enhances the effectiveness of the complementary filter in subsequent processing steps.

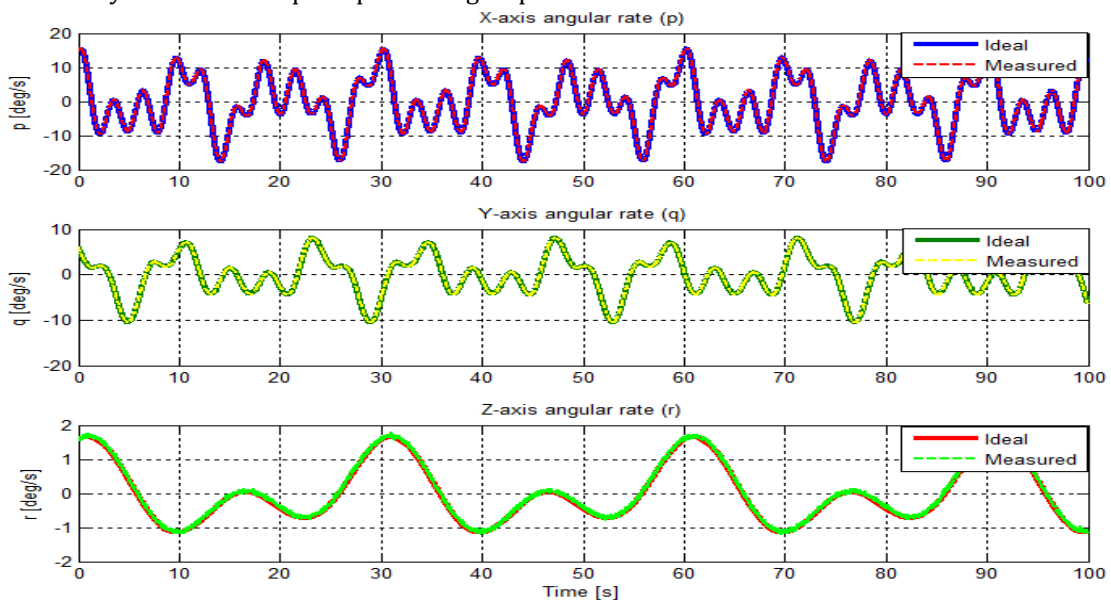


Figure 4. Ideal and measured angular velocities on three axes

Figure 4 compares the ideal angular velocities (Ideal) with the measured angular velocities (Measured) from the gyroscope on the three axes p, q, r . Results show:

For roll rate (p): measured signals closely track the ideal value, though small deviations exist due to noise and bias. The overall oscillation is accurately reproduced, showing that gyros have high sensitivity to rapid motion variations.

For pitch rate (q): the main oscillation trend is captured, but random error is more noticeable, consistent with the fact that the pitch axis is more influenced by wave noise and sensor disturbances.

For yaw rate (r): measured and ideal data almost coincide, with only very small deviations. Since yaw angular velocity amplitude is much smaller than roll and pitch, bias drift has less effect in the short term.

In summary, Figure 4 shows that gyroscope data have high quality in simulating ship dynamics, but still contain inherent noise and bias drift. This explains why the gyro-only method suffers cumulative errors when estimating Euler angles and emphasizes the importance of combining accelerometer data in the complementary filter.

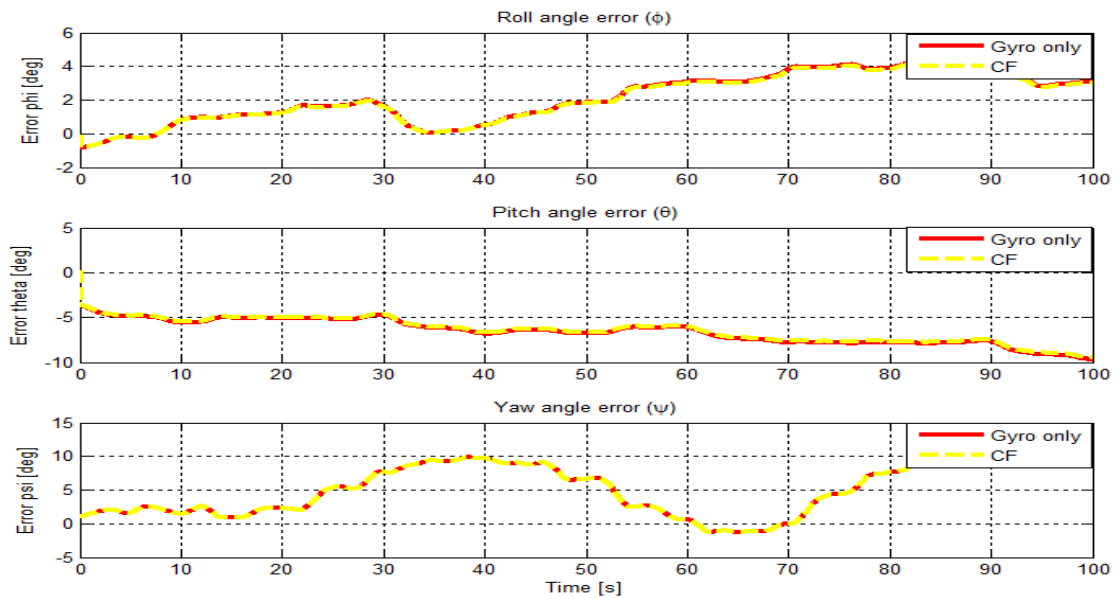


Figure 5. Euler angle errors between Gyro-only and Complementary Filter (CF)

Figure 5 presents the estimation errors of the three Euler angles (roll, pitch, yaw) when using the two methods: gyro integration only (Gyro-only) and complementary filter (CF). Observations are as follows:

For roll (ϕ): gyro-only error increases over time, showing clear drift accumulation. CF limits this drift, maintaining errors within ± 2 (deg), demonstrating the correction role of the accelerometer.

For pitch (θ): gyro-only error exhibits a significant negative bias (around -8 (deg) to -5 (deg)). CF corrects part of this bias but not completely, still maintaining much smaller and more stable errors than gyro-only.

For yaw (ψ): both methods show increasing errors over time, reaching nearly 15 (deg) after 100 (s). Since CF does not use accelerometer for yaw correction, the result is almost identical to gyro-only, still heavily affected by gyro drift.

The results in Figure 5 confirm that CF is clearly effective in reducing roll and pitch errors. However, for yaw, it is necessary to integrate additional magnetometer sensors or use more advanced orientation algorithms to improve accuracy. This is fully consistent with the research direction of the paper, emphasizing the role of the complementary filter in ship orientation systems operating in rough seas.

4. Conclusion

This paper has proposed and verified a method for estimating ship Euler angles (roll, pitch, yaw) based on a multi-frequency wave model and a complementary filter. The novelty of this study lies in employing the multi-frequency wave model to accurately simulate the complex oscillatory characteristics of ships in rough sea conditions, thereby generating highly realistic test data. At the same time, the complementary filter is applied to combine the advantages of the gyroscope (high sensitivity, fast response) and the accelerometer (long-term stability, no drift), improving the reliability of the estimation results.

Simulation results show that the proposed method significantly reduces errors compared to the gyro-only approach, particularly for roll and pitch angles, while maintaining stability in noisy environments. Although yaw angle remains affected by gyro drift, the study points out the extension direction of incorporating magnetometer data to improve performance. Thus, the proposed method is both feasible and

highly accurate, promising effective application in ship navigation and control systems operating in rough seas. The next research direction is to incorporate simulated pseudo linear accelerations into the accelerometer data. Building on the established multi-frequency wave model, the study will be extended by including acceleration components caused by ship body motions such as heave, surge, and sway. These components are unrelated to gravity but appear in real accelerometer data, causing significant deviations when computing angles from sensors. In particular, linear accelerations can be modeled as colored noise or band-limited random signals, accurately reflecting the characteristics of rough sea environments. The inclusion of this factor aims to create conditions for the estimation algorithm to handle “pseudo-noise” similar to reality, thereby assessing the robustness and adaptability of the proposed method under complex dynamic influences.

Declaration of Conflicting Interests

The authors declare no potential conflicts of interest with respect to the research, authorship and publication of this article.

Funding

The author received no financial support for the research, authorship and publication of this article.

References

- [1] Y. Shi, Y. Zhang, Z. Li, S. Yuan, and S. Zhu, “IMU/UWB fusion method using a complementary filter and a Kalman filter for hybrid upper limb motion estimation,” *Sensors*, vol. 23, no. 15, 2023.
- [2] O. Uyar, “Performance evaluation of IMU filtering techniques in yaw-pitch-roll calculations,” *International Journal of Advanced Natural Sciences and Engineering Researches*, vol. 8, 2024.
- [3] Ö. Karal and H. Kazdal, “A new fuzzy logic-based adaptive complementary filter algorithm for UAV attitude estimation,” *Pamukkale University Journal of Engineering Sciences*, vol. 30, no. 3, 2024.
- [4] A. Liu, H. Guo, M. Yu, J. Xiong, H. Liu, and P. Xie, “Research on GNSS/IMU/Visual fusion positioning based on adaptive filtering,” *Applied Sciences*, vol. 14, 2024.
- [5] K. Ghanizadegan and H. A. Hashim, “Quaternion-based unscented Kalman filter for 6-DoF vision-based inertial navigation in GPS-denied regions,” *arXiv preprint*, 2024.
- [6] H. A. Hashim, A. E. E. Eltoukhy, and K. G. Vamvoudakis, “UWB ranging and IMU data fusion: nonlinear stochastic filter for inertial navigation,” *arXiv preprint*, 2023.
- [7] J. Perez, A. Jimenez, and F. Torres, “Ship attitude estimation using inertial sensors and sensor fusion techniques,” *Ocean Engineering*, vol. 148, pp. 497–509, 2018.
- [8] T. I. Fossen, *Handbook of Marine Craft Hydrodynamics and Motion Control*, 2nd ed., Wiley, 2021.
- [9] H. Fourati, “Heterogeneous data fusion algorithm for pedestrian navigation via foot-mounted inertial sensors,” *IEEE Sensors Journal*, vol. 15, no. 8, pp. 4317–4328, 2015.
- [10] J. B. Kuipers, *Quaternions and Rotation Sequences: A Primer with Applications to Orbits, Aerospace and Virtual Reality*, Princeton University Press, 2017.